Numerical evaluation of surface settlement induced by shield tunneling at rock mass

Jun-Beom An
Korea Advanced Institute of Science and Technology, Daejeon, Rep. of Korea

Jeonguk Bang
Korea Advanced Institute of Science and Technology, Daejeon, Rep. of Korea

Joo-Hyun Seong
Korea Advanced Institute of Science and Technology, Daejeon, Rep. of Korea

Gye-Chun Cho
Korea Advanced Institute of Science and Technology, Daejeon, Rep. of Korea

ABSTRACT: There are several precedents of unintended surface settlements resulting in enormous loss of costs and time, even if for the rock medium. The expansion of shield tunneling requires controlling the shield tunneling parameters precisely to reduce the surface settlements. In this study, numerical parametric studies are conducted to evaluate the geotechnical properties, and TBM operational factors on the surface settlements during shield tunneling. The numerical model based on FLAC3D is validated by comparing the results with the literature and field data. Ground stiffness is the dominant factor in the settlement, and the groundwater inflow follows it. The face pressure and tail void grouting pressure show a relatively weak impact on surface settlements because of the higher stiffness of rock mass. The results from this study are expected to contribute to understanding the settlement behavior induced by shield tunneling through the rock mass and the prediction of surface settlement.

Keywords: shield tunneling, surface settlement, groundwater inflow, face pressure, tail void grouting.

1 INTRODUCTION

Shield tunneling has been extensively applied in urban areas since it can achieve tunnel construction with minimized ground deformation by continuous excavation and support. However, there are several precedents of unintended surface settlements resulting in enormous loss of costs and time, even if for the rock medium. The expansion of shield tunneling requires controlling the shield TBM precisely to reduce the surface settlement. The parameters triggering the surface settlement during the shield tunneling vary; tunnel geometry factors such as the diameter and depth of the tunnel (Melis et al. 2002 and Chakeri et al. 2013), ground properties such as the elastic modulus, cohesion, and unit weight (Selby 1988 and Golpasand et al. 2018), the operational factors such as face pressures and steering gap slurry pressures (Lambrughi et al. 2012 and Comodromos et al. 2014), tail void grouting pressure, the amount of backfills and injection point (Suwansawat & Einstein 2007 and Kim et al. 2018), and other mechanical data from Tunnel Boring Machines (TBMs) (Goh & Hefney 2010 and Kim et al. 2020). All these factors are related to unavoidable gaps or stress imbalances. Among

them, the operator can regulate only the support pressure on the tunnel face, along the shield skin, and along the annular between excavated surface and segmental linings. However, the surface settlements that are not directly governed by the pressure balance can be caused by direct ground loss such as the failure of achieving impermeability. As the groundwater inflows during tunneling, it causes the groundwater drawdown resulting in the reduction in pore pressure, which means the increasing effective stress, and the seepage forces occurred at the path of groundwater flow causes the ground deformation locally (Yoo 2016). In this study, several numerical parametric studies are conducted to evaluate the impact of geotechnical properties and TBM operational factors on the surface settlements during shield tunneling. The numerical model based on FLAC3D is validated by comparing the results with the literature and field data. The operational factors selected for parametric studies are face pressure, tail void grouting injection pressure, and groundwater inflow regarding the grout's setting time. It is expected that the order and amount of contribution to the surface settlement can help to understand the settlement behavior induced by shield tunneling through the rock mass in a realistic view.

2 SURFACE SETTLEMENT INDUCED BY SHIELD TUNNELING

The settlement induced by shield tunneling showed settlement trough at the surface above tunnel. The transverse settlement trough has been illustrated to follow a Gaussian distribution curve (Peck 1969 and O'Reilly & New 1982). The Gaussian distribution curve is plotted using the equation as shown below:

$$S = S_{max} \cdot exp\left(\frac{-y^2}{2i^2}\right) \quad (1)$$

where S is the settlement at the point y, S_{max} is the maximum settlement at the tunnel centerline, y is the distance from the tunnel centerline, and the i is the distance from the tunnel centerline to the inflection point of the trough. The inflection point can be assumed with respect to the product of the depth of tunnel z_0 and trough width parameter K (O'Reilly & New 1982). Mair & Taylor (1997) investigated the value of trough width parameter as 0.5 for clays and 0.35 for sands or gravel based on field data.

3 NUMERICAL MODELING

A numerical analysis is carried out based on the finite difference method (FDM) using the commercial software FLAC3D developed by Itasca.

3.1 Modeling of the ground

The size of the domain is determined to describe the ground in accordance with an infinite medium, such that the boundary effect is neglected (Lambrughi et al. 2012). The domain is 120m in the longitudinal direction of excavation, 90m from the tunnel axis in the transverse direction, and 60m for the mesh height. The zone elements are applied for the ground, and the roller boundary is adopted. The nodes at all side except upper surface are fixed in the orthogonal direction.

The geotechnical properties are selected to adopt the Mohr-Coulomb failure criterion, which is assumed that well matched with typical rock mass. It is required that the bulk modulus, shear modulus, internal friction angle, cohesion, and density for each layer. In addition to the mechanical model, the hydraulic properties are also required such as the permeability, porosity, and the Biot coefficient. The Biot coefficient is a parameter that determines the level of attenuation of pore fluid pressure. In the case of saturated soils, the soil particles are considered as incompressible and the soil matrix will be deformed for increasing confining stress. It is because the bulk modulus of water is much higher than that of soil minerals. However, for the porous rock medium, the rock skeleton can

be stronger than the pore water. Thus, the stress is shared with following the Biot coefficient and the effective stress is increased.

The initial condition of the ground is calculated iteratively until the mechanical ratio between the unbalanced forces reached below 1e-05 after the ground properties and gravitational force are designated.

3.2 Modeling of the structural elements

Structures such as shield, lining segments, and backfill grouts are simulated by shell elements with a linear elastic model (Comodromos et al. 2014 and Moeinossadat and Ahangari 2019). The zone elements overlapped the shell elements except shield to consider the deformation in the thickness direction. Shield is assumed to have no tapering or steering gaps.

3.3 Modeling of the face pressure

Face pressure is applied in a direction normal to the nodes on the tunnel face. The value follows the horizontal earth pressure at the center of the tunnel. It is described using the face pressure ratio (FPR), which is the ratio between the face pressure and horizontal total earth pressure at rest on the tunnel face. The face pressure value is estimated by following the Japan Geotechnical Society method, for simple and versatile application. Maximum earth pressure is assumed as the earth pressure at rest including pore pressure, and minimum earth pressure is assumed as the Rankine's active earth pressure with pore pressure. Thus, the FPR will be in range 0.6 ~ 1.0 at dry condition, and in range about 0.8 ~ 1.0 at wet condition.

3.4 Modeling of the tail void grouting

The grout injected on the tail void is simulated to be hardened with time. The hardening behavior is following the CEB-FIP model code for a time coefficient β_{cc} as 0.38. For simple calculation, grout hardening is discretely simulated in this study. The average advance of the shield is assumed to be 10 rings per day. 27, 44, 54, 61, 66, 70, 73, 76, 78, 80, 82, and 83 % of the completely hardened modulus is applied at each of the five rings after injection.

The injection pressure on the excavated surface is applied uniformly in a normal direction for up to five rings after injection, assuming that the initial setting time of the grouts is about 12 hrs. The pressure is 100kPa higher than the face pressure, which is in a range recommended in fields. It is also described with backfill injection pressure ratio (BPR), which is a ratio between grout injection pressure and the total earth pressure at rest on the tunnel face. Schematic diagram of numerical modeling including the face pressure and tail void grouting is presented in Fig. 1.

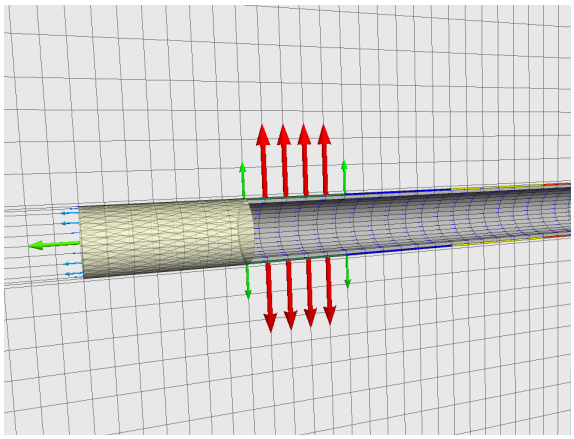

Figure 1. Numerical modeling presenting applied pressure and discretely strengthening grouts.

3.5 Modeling of the shield tunneling process

The shield tunneling is iteratively carried out in sequence by nulling the elements as a unit advance (a ring span), loading the face pressure, creating lining segment and backfill grouts with injection pressure. The face pressure on the former tunnel face is eliminated as the shield advanced. Tail void grouting is conducted by simultaneous injection.

For the undrained excavation, the fluid configuration turned off and it only solves the mechanical calculations. For the groundwater inflow, the mechanical calculation and fluidal calculation are conducted on shifts. It is possible because the perturbation is due to the change in pore pressure, not mechanical process in major. The groundwater inflow requires the time-dependent behavior, while the undrained process does not consider the real time.

3.6 Validation of numerical simulation

The numerical simulation is validated with data combined by excavation along the soil and rock medium. All cases assumes the green-field condition. From the validation below, the numerical simulation used in this study is considered proper for parametric study.

3.6.1 Validation 1. Tehran subway line 7

In this case, the tunnel is constructed by EPB shield TBM which has a diameter of 9.2 m, ring span of 1.5 m (Moeinossadat and Ahangari 2009). The depth of the tunnel is 20.8 m, and it passes through the silty gravel medium without groundwater inflow. The numerical results showed that the maximum settlement is about 6.95 mm, where the measured field value is about 6.9 ~ 7.1 mm.

3.6.2 Validation 2. Utility tunnel in Korea

In this case, the tunnel is constructed by EPB shield TBM which has a diameter of 3.6 m, ring span of 1.2 m. The depth of the tunnel is 42.0 m, the groundwater level is about 2.0 m and it passes through the hard rock medium. The groundwater inflow is assumed to have been occurred by 0.9 m^3/day/m. The numerical results showed that the maximum settlement is about 1.2 ~ 1.4 mm, where the measured field value is about 1 ~ 3 mm.

3.6.3 Validation 3. Tunnel in Korea

In this case, the tunnel is constructed by Single shield TBM which has a diameter of about 5.0 m (Moon & Oh 2022). The ring span is assumed as 1.2 m. The depth of the tunnel is about 42 m, the groundwater level is about 6.0 m, and it passes through the weathered rock medium. The groundwater inflows for a long time without proper impermeable layers. The numerical results showed that the maximum settlement is about 111.3 mm, where the measured field value is about 123.0 mm.

4 RESULTS AND DISCUSSIONS

For the comprehensive evaluation, the results of former study is included (An et al. 2022). With the same numerical domain, the depth of the tunnel is fixed at 20 m. The excavation has a diameter of 3.6 m, shield length of 8.4 m, ring span of 1.2 m, and the external diameter of segment is 3.4 m. The groundwater level is 2.0 m below the surface. The geotechnical properties of weathered rock (WR), soft rock (SR), and hard rock (HR) are tabulated in Table 1.

4.1 Pressure imbalance

The surface settlements decreases with maximum face pressure and large enough grout injection pressure in tail void. However, the settlements induced by pressure imbalance during the shield

tunneling show insignificant differences between FPRs and BPRs. Especially for the hard rock, the rock mass can stand on its own and the stress imbalance does not lead to settlement.

Table 1. Rock mass properties for parametric studies.

	Density [kg/m^3]	Cohesion [kPa]	Internal friction angle [degree]	Elastic modulus [MPa]	Poisson's ratio [-]	Perm-eability [cm/s]	Porosity [-]	Biot coefficient [-]
WR	2,100	30	33	100	0.30	3e-04	0.10	1
SR	2,500	140	37	2,000	0.28	1.03e-04	0.05	0.1
HR	2,800	1,000	45	8,000	0.25	2.24e-05	0.01	0.015

4.2 Groundwater inflow

The settlement mechanism due to the groundwater inflow has two options which occurs simultaneously. The groundwater inflow causes the drawdown resulting in the reduction in pore pressure, which means the increasing effective stress. And the seepage forces occurred at the path of groundwater flow causes the ground deformation locally. Settlements induced by groundwater inflow during the shield tunneling show widened troughs because the hydraulic influence range is larger than mechanical range. As the inflow time getting longer, the maximum settlements increases and converges. The flow speed does not show significant difference because the seepage force driven deformation is comparatively ignorable at rock mass.

Compared with the former study for the settlement induced by undrained excavation, the order of trough parameter for the stiffness is reversed at the case of groundwater inflow occurrence. The settlements are large and narrow at weak weathered rock as shown in Fig. 2a (An et al. 2022), the settlements becomes larger and widened as the groundwater inflow occurs as shown in Fig. 2b. It can be inferred that the horizontal displacement becomes dominant by groundwater flow.

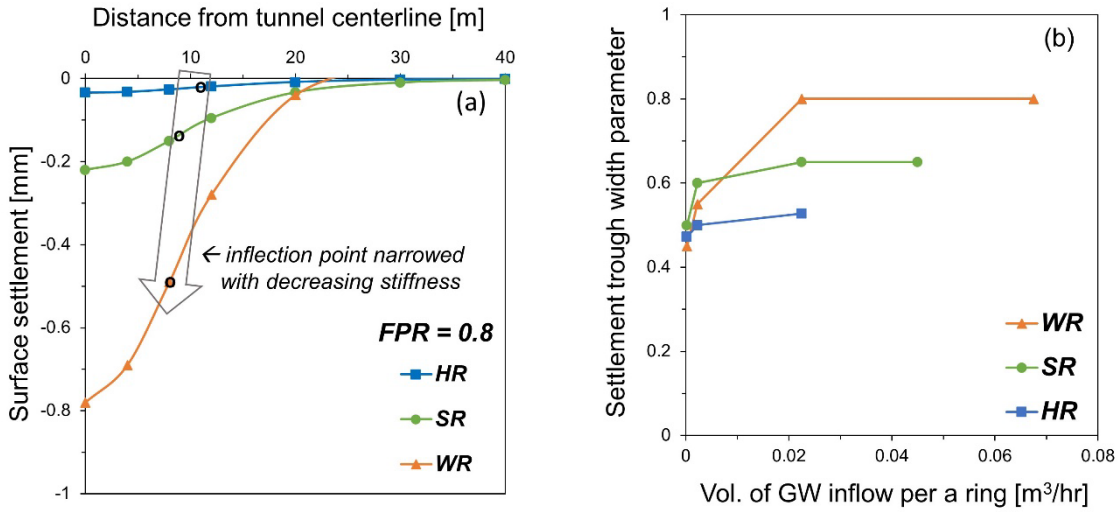

Figure 2. The settlement trough width parameter change for (a) undrained; (b) groundwater inflow.

The pore pressure drop becomes to zero when it goes farther from the tunnel. The drop of pore pressure is definite at the deeper range, while the pore pressure at the upper soil layers are remains. The low permeability of rock mass affects the pore pressure above. If the pore pressure driven deformation is influenced by groundwater drawdown, it starts from upper layer to the lower layer. Therefore, it insists that the groundwater inflow is relatively radial into a deep tunnel (Goodman et al. 1965 and Fernandez 1994).

5 CONCLUSIONS

The numerical simulation is performed to evaluate the surface settlement caused by shield tunneling. It is validated by comparison with the literature and field data. The face pressure, tail void grouting pressure, and the groundwater inflow are studied for the porous rock medium. The parametric studies insist that the ground stiffness is the most governing factor for the surface settlement. Among the operational factors, the installation of impermeable layer on the segment lining is the most crucial on the surface settlement. The stress imbalance are less significant due to the high stiffness of rock mass.

ACKNOWLEDGEMENTS

This research was supported by UNDERGROUND CITY OF THE FUTURE program funded by the Ministry of Science and ICT.

REFERENCES

An, J. B., Kang, S. J., Kim, J., & Cho, G. C. (2022). Numerical evaluation of surface settlement induced by ground loss from the face and annular gap of EPB shield tunneling. *Geomechanics and Engineering* 29 (3), pp. 291-300.

Chakeri, H., Ozcelik, Y., & Unver, B. (2013). Effects of important factors on surface settlement prediction for metro tunnel excavated by EPB. *Tunnelling and Underground Space Technology* 36, pp. 14-23.

Comodromos, E. M., Papadopoulou, M. C., & Konstantinidis, G. K. (2014). Numerical assessment of subsidence and adjacent building movements induced by TBM-EPB tunneling. *Journal of Geotechnical and Geoenvironmental Engineering* 140 (11), 04014061.

Fernandez, G., 1994. Behavior of pressure tunnels and guidelines for liner design. *J. Geotech. Eng. ASCE* 120 (10), pp. 1768–1791.

Golpasand, M. B., Do, N. A., Dias, D., & Nikudel, M. R. (2018). Effect of the lateral earth pressure coefficient on settlements during mechanized tunneling. *Geomech. Eng* 16 (6), pp. 643-654.

Goodman, R., Moye, D., Schalkwyk, A., Javendel, I., 1965. Ground-water inflow during tunnel driving. *Eng. Geol.* 2 (2), pp. 39–56.

Kim, D., Pham, K., Park, S., Oh, J. Y., & Choi, H. (2020). Determination of effective parameters on surface settlement during shield tbm. *Geomechanics and Engineering* 21 (2), pp. 153-164.

Kim, K., Oh, J., Lee, H., Kim, D., & Choi, H. (2018). Critical face pressure and backfill pressure in shield TBM tunneling on soft ground. *Geomechanics and Engineering* 15 (3), pp. 823-831.

Lambrughi, A., Rodríguez, L. M., & Castellanza, R. (2012). Development and validation of a 3D numerical model for TBM–EPB mechanised excavations. *Computers and Geotechnics* 40, pp. 97-113.

Mair, R. J., & Taylor, R. N. (1997, September). Theme lecture: Bored tunnelling in the urban environment. In *Proceedings of the fourteenth international conference on soil mechanics and foundation engineering,* pp. 2353-2385, Rotterdam.

Melis, M., Medina, L., & Rodríguez, J. M. (2002). Prediction and analysis of subsidence induced by shield tunnelling in the Madrid Metro extension. *Canadian Geotechnical Journal* 39 (6), pp. 1273-1287.

Moeinossadat, S. R., & Ahangari, K. (2019). Estimating maximum surface settlement due to EPBM tunneling by Numerical-Intelligent approach–A case study: Tehran subway line 7. *Transportation Geotechnics* 18, pp. 92-102.

O'Reilly, M. P., & New, B. M. (1982). Settlements above tunnels in the United Kingdom-their magnitude and prediction (No. Monograph).

Peck, R. B. (1969). Deep Excavations and Tunneling in Soft Ground. *Proc. 7th ICSMFE, State of the Art Volume*, pp. 225-290.

Selby, A. R. (1988). Surface movements caused by tunnelling in two-layer soil. *Geological Society, London, Engineering Geology Special Publications* 5 (1), pp. 71-77.

Suwansawat, S., & Einstein, H. H. (2007). Describing settlement troughs over twin tunnels using a superposition technique. *Journal of geotechnical and geoenvironmental engineering* 133(4), pp. 445-468.